

# APPARATUS AND DEMONSTRATION NOTES

Frank L. H. Wolfs, *Editor*

*Department of Physics and Astronomy, University of Rochester, Rochester, New York 14627*

This department welcomes brief communications reporting new demonstrations, laboratory equipment, techniques, or materials of interest to teachers of physics. Notes on new applications of older apparatus, measurements supplementing data supplied by manufacturers, information which, while not new, is not generally known, procurement information, and news about apparatus under development may be suitable for publication in this section. Neither the *American Journal of Physics* nor the Editors assume responsibility for the correctness of the information presented.

Manuscripts should be submitted using the web-based system that can be accessed via the *American Journal of Physics* home page, <http://www.kzoo.edu/ajp/> and will be forwarded to the ADN editor for consideration.

---

## An audible demonstration of the speed of sound in bubbly liquids

Preston S. Wilson<sup>a)</sup>

*Mechanical Engineering Department and Applied Research Laboratories, The University of Texas at Austin, Austin, Texas 78712-0292*

Ronald A. Roy

*Department of Aerospace and Mechanical Engineering, Boston University, Boston, Massachusetts 02215*

(Received 5 January 2007; accepted 18 March 2008)

The speed of sound in a bubbly liquid is strongly dependent upon the volume fraction of the gas phase, the bubble size distribution, and the frequency of the acoustic excitation. At sufficiently low frequencies, the speed of sound depends primarily on the gas volume fraction. This effect can be audibly demonstrated using a one-dimensional acoustic waveguide, in which the flow rate of air bubbles injected into a water-filled tube is varied by the user. The normal modes of the waveguide are excited by the sound of the bubbles being injected into the tube. As the flow rate is varied, the speed of sound varies as well, and hence, the resonance frequencies shift. This can be clearly heard through the use of an amplified hydrophone and the user can create aesthetically pleasing and even musical sounds. In addition, the apparatus can be used to verify a simple mathematical model known as Wood's equation that relates the speed of sound of a bubbly liquid to its void fraction. © 2008 American Association of Physics Teachers.

[DOI: 10.1119/1.2907773]

### I. INTRODUCTION

The interaction of sound and bubbles has been studied in modern science for almost 100 years and has been part of human consciousness for many hundreds of years, perhaps longer. It is a scientifically interesting and complex phenomenon with a long and diverse history, yet our understanding of the phenomenon is still incomplete. Part of the intrigue comes from the fact that minute parameter changes in a bubbly fluid can have large and unexpected effects. For example, consider a column of water contained within a rigid tube. The addition of just a small number of bubbles, representing as little as 0.1% by volume, can transform the once simple medium into a highly dispersive and nonlinear one, with a speed of sound less than 20% of the speed of sound in the host medium. That corresponds to a 4 parts in 5 change in the speed of sound for a 1 part in 10 000 change in the density. It is the added compressibility of the gas phase that causes the reduction of the speed of sound.

The early scientific work on the acoustics of bubbles was motivated primarily by the desire to understand certain man-made and natural curiosities. In 1910, a paper was published by Mallock<sup>1</sup> that sought to explain the fact that when struck,

a drinking glass filled with a “frothy liquid” produces a dull sound. Perhaps inspired by his former laboratory assistant,<sup>2</sup> Rayleigh published a paper in 1917 that described the sound produced by water boiling in a tea kettle.<sup>3</sup> In 1933, Minnaert studied the sounds produced by running water, such as the flowing stream and the crashing of ocean waves.<sup>4</sup> The latter two studies both introduced relationships between the size of a bubble and its period of oscillation with water as the host medium, but Rayleigh considered steam bubbles while Minnaert considered air bubbles.

The acoustics of bubbly liquids now has a number of important practical applications. These include a variety of industrial processes utilizing multiphase flow,<sup>5</sup> microfluidic manipulation,<sup>6</sup> and the design of nuclear reactor containment systems.<sup>7</sup> In the ocean, various acoustic techniques are used in conjunction with oceanic bubble populations to make measurements relevant to meteorology, chemical oceanography, marine fluid dynamics, and marine biology.<sup>8</sup> By shrouding propellers and hulls with man-made bubble screens, unwanted noise produced by ships and submarines is reduced.<sup>9</sup> Bubbles are used in medical applications to enhance ultrasound imaging,<sup>10</sup> hemostasis,<sup>11</sup> and therapy.<sup>12</sup>

Both theory and measurement reveal that for acoustic ex-

citation frequencies that are close to the individual bubble resonance frequency, the acoustic attenuation within a bubbly liquid is measured in tens of decibels per centimeter, and that the sound speed can vary from as little as 20 m/s to as much as 10 000 m/s, which is supersonic relative to bubble-free water. In the littoral ocean environment, this behavior is a dominant obstacle for effective sonar operation because bubbles and bubble clouds are produced in abundance by breaking waves. The acoustic contrast provided by bubbly liquid causes sound to be scattered from bubble clouds, and hence naval sonar and mine hunting operations are hindered.

Bubbles are also a source of ambient noise in the ocean. Rain drops, spray from breaking waves, and even snow can entrain bubbles when they impact the ocean surface. The impact deforms the ocean surface and creates an air cavity. When this cavity closes, a bubble is formed and a second impact that occurs when the air cavity closes causes the bubble to oscillate and radiate sound.<sup>13–15</sup> Breaking waves produce clouds composed of large numbers of bubbles that oscillate collectively and radiate sound. These bubble clouds are responsible for part of the ambient noise in the ocean below about 1000 Hz.<sup>16</sup>

The physics of bubble acoustics has been the subject of previous “Apparatus and Demonstration Notes” within this journal,<sup>17–19</sup> but the apparatus described here complements and expands upon the previous work. The apparatus consists of a transparent PVC pipe about 0.5 m in length. Air bubbles are injected at the bottom of the water-filled tube and a hydrophone is used to detect the resulting sounds. The apparatus can be used to demonstrate the bubble sound production mechanism and the bubbly liquid’s speed of sound dependence on the air/water volume fraction. The latter is observed indirectly via the pitch of the sound. If the sounds are recorded, the data can be used to verify Wood’s equation, which is a mathematical model that relates the speed of sound in a bubbly liquid to the fractional volume of air.

This demonstration has been conducted for audiences ranging from professional acousticians to prospective undergraduate students and their parents. It is always a hit and usually generates questions and discussion. The basic theory governing bubble oscillation, sound propagation in bubbly liquids, and the acoustics of one-dimensional waveguides is presented in Sec. II. The demonstration apparatus is described in Sec. III. In Sec. IV the use of the apparatus is described. Finally, the technique used to verify Wood’s equation with our apparatus is discussed in Sec. V.

## II. THEORETICAL CONSIDERATIONS

Consider a spherical air bubble with equilibrium radius  $\bar{a}$  suspended in a liquid at room conditions: atmospheric pressure and 20 °C. For  $\bar{a} > 10 \mu\text{m}$ , the surface tension and vapor pressure can be ignored and the hydrostatic pressure of the surrounding water is balanced by the gas pressure inside the bubble. Assuming the air is an ideal gas, it is governed by the relation

$$PV^\nu = \text{constant}, \quad (1)$$

where  $P$  is the pressure,  $V$  is the volume, and  $\nu$  is the polytropic index. For air bubbles in water, the value of  $\nu$  can range from  $\nu = \gamma$ , where  $\gamma$  is the ratio of specific heats of the air, to  $\nu = 1$ . These limits bound a continuum of behavior that ranges from adiabatic to isothermal, depending on the bubble size and the frequency of excitation.

If the bubble radius is perturbed, equilibrium is lost and oscillations occur. The alternating compression and expansion of the bubble is due to the transfer of energy between the inertia provided by the surrounding liquid and the compressibility of the gas inside the bubble. For the frequency range between 100 and 1200 Hz and a bubble size of about 1 mm, it is sufficient to assume lossless conditions within the bubble, but dissipative effects are important in other regimes.<sup>20</sup> At a hydrostatic pressure  $P_\infty$ , the compressibility of the gas inside the bubble leads to an effective stiffness  $12\pi\bar{a}\nu P_\infty$ .<sup>21</sup> The bubble behaves acoustically like a pulsating sphere and radiates sound uniformly in all directions. Since the bubble size is always much smaller than the resulting acoustic wavelength, the low frequency limiting value of the acoustic radiation reactance can be used to define an effective mass, known as the radiation mass  $4\pi\bar{a}^3\rho_\ell$ , where  $\rho_\ell$  is the liquid density. The bubble’s resonance frequency is then given by the square root of the stiffness to mass ratio, or

$$\omega_0 = \frac{1}{\bar{a}} \sqrt{\frac{3\nu P_\infty}{\rho_\ell}} \quad (\text{radians/sec}). \quad (2)$$

This relation was first derived by Minnaert<sup>4</sup> in 1933, although via a different methodology. Minnaert considered bubbles in the size range between 3 and 6 mm, and concluded that the period of oscillation would be small compared to the time required for the heat of compression to be conducted away. The bubble was considered to be undergoing an adiabatic process, and hence the polytropic index  $\nu$  was taken to be the ratio of specific heats  $\gamma$ .

The assumption of adiabatic behavior made by Minnaert was reasonable for the bubble sizes he was considering, but it is instructive to consider a more accurate description. Leighton<sup>22</sup> considered bubbles undergoing natural oscillation and those driven by an external acoustic field, and showed that because of the high thermal conductivity and specific heat capacity of the surrounding liquid, the gas in direct contact with the bubble wall can be considered isothermal. The gas at the center of the bubble behaves adiabatically. Therefore, the effective polytropic index for the bubble as a whole can take on a range of intermediate values depending on the bubble’s size relative to the size of the thermal boundary layer. The ratio of the bubble equilibrium radius to the length of thermal boundary layer  $l_{\text{th}}$  is given by

$$\frac{\bar{a}}{l_{\text{th}}} = \frac{\bar{a}\sqrt{2\omega}}{\sqrt{D_g}}, \quad (3)$$

where  $D_g$  is the thermal diffusivity of the gas and  $\omega$  is the frequency of excitation.<sup>22</sup> At sufficiently high frequencies, the bubble is much larger than  $l_{\text{th}}$  and it behaves adiabatically. At sufficiently low frequencies, the bubble is much smaller than  $l_{\text{th}}$  and it behaves isothermally. The value of  $D_g$  for air at room temperature is  $2.08 \times 10^{-5} \text{ m}^2/\text{s}$ , and therefore  $\bar{a} \approx 90l_{\text{th}}$  for Minnaert’s bubbles, confirming the adiabatic assumption.

### A. Low frequency sound propagation in bubbly liquids

Now consider propagation of sound through a collection of bubbles, where the incident acoustic pressure is the source of the perturbations. In 1910 Mallock<sup>1</sup> applied mixture theory to what he termed “frothy liquids,” under the assumption that the gas bubbles were of such number and separation that the medium could be considered homogenous, and he

obtained an approximate expression for the speed of sound in the bubbly liquid. In 1930, Wood<sup>23</sup> began with a thermodynamic argument and confirmed Mallock's work, but cast the results in a more useful form, and specifically considered air bubbles in water. In this section, the equation governing the low-frequency speed of sound in bubbly liquids is developed, based on the work of Wood.<sup>23</sup>

The following assumptions and definitions are used. The bubbly fluid is composed solely of spherical gas bubbles suspended in liquid under the influence of acoustic pressure fluctuations. The subscripts  $\ell$  and  $g$  refer to the liquid and gas phases, respectively. Effective quantities pertaining to the mixture are denoted with the subscript  $m$ . Mass is conserved such that the mixture mass is the sum of the liquid and gas masses, with no relative translational motion between the two phases. The volume fraction of the gas phase, known as the void fraction  $\chi$ , is given by

$$\chi = V_g/V_m, \quad (4)$$

where  $V_g$  is the volume of the gas phase and  $V_m$  is the total volume of the mixture, given by  $V_m = V_g + V_\ell$ . The effective mixture density is

$$\rho_m = (1 - \chi)\rho_\ell + \chi\rho_g, \quad (5)$$

where  $\rho_\ell$  is the density of the liquid and  $\rho_g$  is the density of the gas. The mixture compressibility  $\kappa_m$  is

$$\kappa_m = (1 - \chi)\kappa_\ell + \chi\kappa_b, \quad (6)$$

where  $\kappa_\ell$  is the compressibility of the liquid and  $\kappa_b$  is the compressibility due to the gas in the bubbles. In general, the speed of sound  $c$  is defined as

$$c^2 = \frac{1}{\rho\kappa}. \quad (7)$$

The value of  $\kappa_b$  and the way it is eventually included in Eq. (7) depends in part upon the conditions that prevail during the compression phase. For air bubbles in water at frequencies that approach zero, the process can be considered isothermal, as was shown rigorously by Hsieh and Plesset.<sup>24</sup> The response of an individual bubble is dominated by the compressibility of the gas within the bubble, hence  $\kappa_b = (\kappa_g)_{\text{isothermal}} = (\nu P_\infty)^{-1}$  with  $\nu = 1$ . As the excitation frequency approaches the bubble resonance frequency, the dynamics of the bubble become important and  $\kappa_b \rightarrow \kappa_b(f) \neq \kappa_g$ . Well above resonance, the bubbles behave adiabatically and  $\kappa_b = (\kappa_g)_{\text{adiabatic}} = (\nu P_\infty)^{-1}$  with  $\nu = \gamma = 1.4$  for air. In between, the polytropic index that governs the compression and expansion of the gas inside the bubbles is frequency dependent, as shown by Prosperetti,<sup>25</sup> and is given by  $\nu = \text{Re}[\Phi]/3$ , where

$$\Phi = \frac{3\gamma}{1 - 3(\gamma - 1)iX[(i/X)^{1/2} \coth(i/X)^{1/2} - 1]} \quad (8)$$

and

$$X = D_g/\omega a^2. \quad (9)$$

In this work, the excitation frequency is well below the bubble resonance, therefore  $\kappa_b = \kappa_g$ . In the frequency range between 200 and 1000 Hz and a bubble size of about 1.0 mm, Eq. (8) yields  $1.26 < \nu < 1.33$ . It is sufficient for our purposes to take the average value of  $\nu$  and set the compressibility of the gas to be

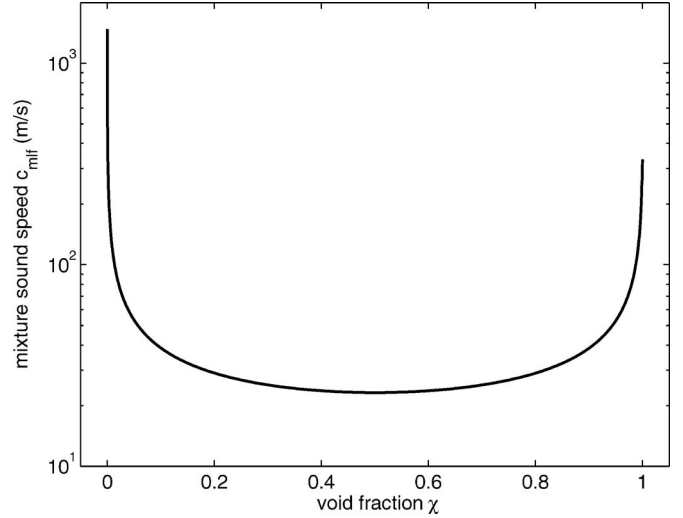


Fig. 1. The low-frequency speed of sound of sounds of bubbly liquid given by Wood's equation [Eq. (12)] for air bubbles in water, with  $\rho_\ell = 998 \text{ kg/m}^3$ ,  $\rho_g = 1.21 \text{ kg/m}^3$ ,  $c_\ell = 1481 \text{ m/s}$  and  $c_g = 333 \text{ m/s}$ . At zero void fraction, the speed of sound is that of the liquid alone. At unity void fraction, the speed of sound is that of the gas alone. The minimum speed of sound is about 23 m/s and occurs at  $\chi = 0.5$ .

$$\kappa_g = \frac{1}{\nu P_\infty} = \frac{1}{1.3 P_\infty}. \quad (10)$$

Substitution of Eqs. (5) and (6) into Eq. (7) results in an equation for the mixture sound speed,

$$\frac{1}{c_m^2} = [(1 - \chi)\rho_\ell + \chi\rho_g][(1 - \chi)\kappa_\ell + \chi\kappa_g], \quad (11)$$

which is equivalent to Wood's 1930 equation.<sup>23</sup> For bubbles well below resonance size where surface tension and dissipative effects are negligible, Eqs. (7) and (10) can be used to relate the previous result to the density and speeds of sound of the two mixture components. After manipulation this results in the equivalent relation

$$\frac{1}{c_{\text{mlf}}^2} = \frac{(1 - \chi)^2}{c_\ell^2} + \frac{\chi^2}{c_g^2} + \chi(1 - \chi) \frac{\rho_g^2 c_g^2 + \rho_\ell^2 c_\ell^2}{\rho_\ell \rho_g c_\ell^2 c_g^2}, \quad (12)$$

where  $c_{\text{mlf}}$  is the low-frequency speed of sound of the mixture. The behavior of Eq. (12) for air bubbles in distilled water is shown in Fig. 1. Note that as the mixture approaches pure liquid,  $\chi \rightarrow 0$  and  $c_{\text{mlf}} \rightarrow c_\ell$ . Alternatively, as  $\chi \rightarrow 1$ ,  $c_{\text{mlf}} \rightarrow c_g$ . Upon approach to  $\chi = 1$ , a change to the adiabatic speed of sound in air would be required. The speed of sound in bubbly liquid, given by Eq. (11) or (12), is known as Wood's low-frequency speed of sound or the Wood limit of the speed of sound.

A minimum occurs at  $\chi = 0.5$ , the speed of sound is lower than the intrinsic speeds of sound in air or water across much of the void fraction range. This remarkable result can be qualitatively explained: bubbles greatly increase the mixture compressibility yet effect the density much less. High compressibility and high density yields a low speed of sound. Another interesting result is that in this regime, the bubble size does not play a role. The primary environmental variable is the void fraction.

Because of the great difference in density and speed of sound between air and water, Eq. (12) can be approximated

by a much simpler expression for a limited range of  $\chi$ . For air bubbles in water, in the range  $0.002 < \chi < 0.94$ , the first two terms on the right-hand side of Eq. (12) are much smaller than the third term. Neglecting them and noting that  $\rho_g^2 c_g^2 \ll \rho_l^2 c_l^2$  results in

$$c_{\text{mlf}}^2 \approx \frac{1}{\rho_l \kappa_g \chi (1 - \chi)}. \quad (13)$$

Substitution of Eq. (10) into Eq. (13) results in a simple approximate expression for the low-frequency speed of sound of the mixture

$$c_{\text{mlf}} \approx \sqrt{\frac{\nu P_\infty}{\rho_l \chi (1 - \chi)}}, \quad (14)$$

and differs less than 1.2% from Eq. (12). Extensions to Eq. (14) accounting for relative motion between the phases, i.e., bubbly fluid flows, have been provided by Crespo<sup>26</sup> and Ruggles *et al.*<sup>27</sup>

### B. Mode shapes and eigenfrequencies of a one-dimensional waveguide

The compressibility of a bubbly liquid is large in comparison to the pipe wall material; hence, the waveguide walls appear effectively rigid. The top of the tube is a water-air interface, hence it is approximated as a pressure release boundary, with  $p=0$ . Again, because of the high compressibility of the bubbly liquid inside the tube, the water just below the opening of the needles appears as a rigid surface, with  $\partial p / \partial x = 0$ . Consider a rigid tube of length  $L$  and circular cross section with radius  $b$ , filled with a fluid possessing a speed of sound  $c_0$ . The cutoff frequency of the lowest order transverse mode is given by<sup>28</sup>

$$f_{11}^c = \frac{\alpha'_{11} c_0}{2\pi b}, \quad (15)$$

where  $\alpha'_{11} = 1.841$  and is the first root of  $J'_1(x)$ , the Bessel function of the first kind of order one, and the prime indicates the derivative with respect to the function's argument. At frequencies below  $f_{11}^c$ , only plane waves can propagate within the tube. Solving the wave equation within this tube for the given boundary conditions yields the eigenfunctions

$$p_n(x) = a_n \cos \frac{\pi(n + 1/2)x}{L}, \quad (16)$$

and eigenfrequencies

$$f_n = \frac{c_0}{2L} (n + 1/2), \quad n = 0, 1, 2, \dots \quad (17)$$

The resonance frequency  $f_n$  is a linear function of the mode number  $n$  with the sound speed  $c_0$  as a parameter.

### III. DESCRIPTION OF DEMONSTRATION APPARATUS

The apparatus, shown in Fig. 2, consists of five basic parts: an acoustic waveguide that is filled with bubbly water, an air injection system that creates the bubbles, a hydrophone that senses the acoustic pressure within the waveguide, a data acquisition system that records and displays the hydrophone signal, and an amplified loudspeaker system that broadcasts the hydrophone signal to the audience.

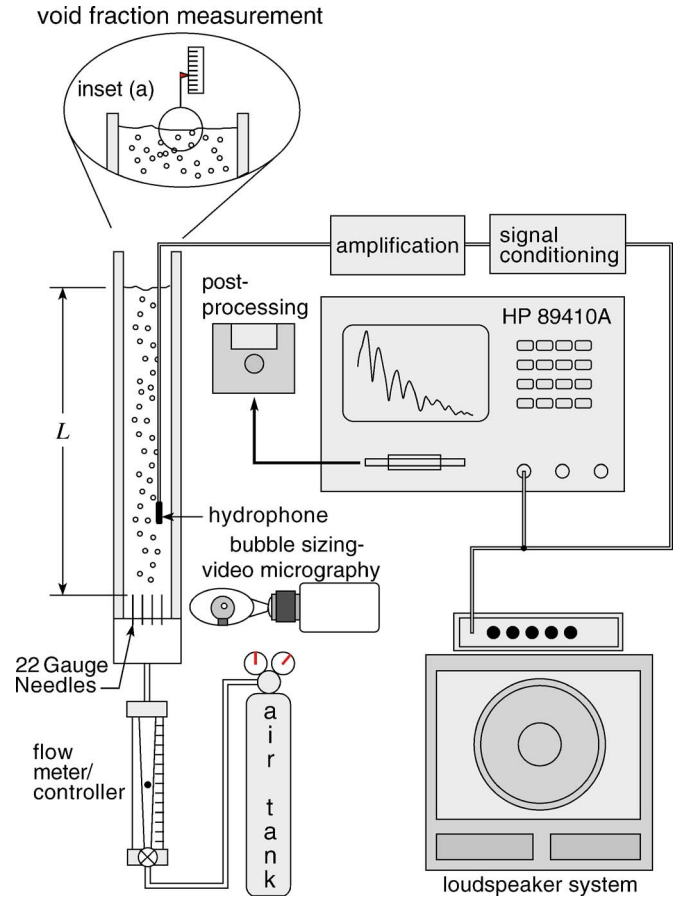


Fig. 2. A schematic of the demonstration apparatus.

The acoustic waveguide was constructed from transparent schedule 40 PVC pipe that is available from plumbing supply houses. The inside diameter was 5.2 cm and the length was 0.6 m. The pipe is typically filled with distilled water to a level of  $\approx 0.5$  m. A bubble injection manifold was fabricated with 12 22-gauge needles<sup>29</sup> embedded in an epoxy filled PVC pipe fitting that attached to the bottom of the pipe. The needles were positioned in a vertical orientation and therefore released air bubbles directly upward. A small mechanical float was positioned at the top of the pipe, such that it floated on the upper surface of the water, as shown in inset (a) of Fig. 2. The float was attached to a pointer that indicated the height of the water surface on a centimeter scale. The overall length  $L$  of the water column in the tube could be measured to an accuracy of about 1 mm. The void fraction is

$$\chi = \Delta \ell / (\ell + \Delta \ell) = \Delta \ell / L, \quad (18)$$

where  $\ell$  is the length of the water column in the absence of bubbles and  $\Delta \ell$  is the change in length when bubbles are present.

Any convenient source of air can be used, as long as the flow rate can be controlled by the user. In our implementation, a canister of medical air was used. The air was directed through a flow meter with a needle valve to control the flow rate, although a measurement of the flow rate is not required. If available, one can use a video camera with a macro (close-up) lens to observe the bubbles and hence determine the bubble size. A typical bubble is shown in Fig. 3.

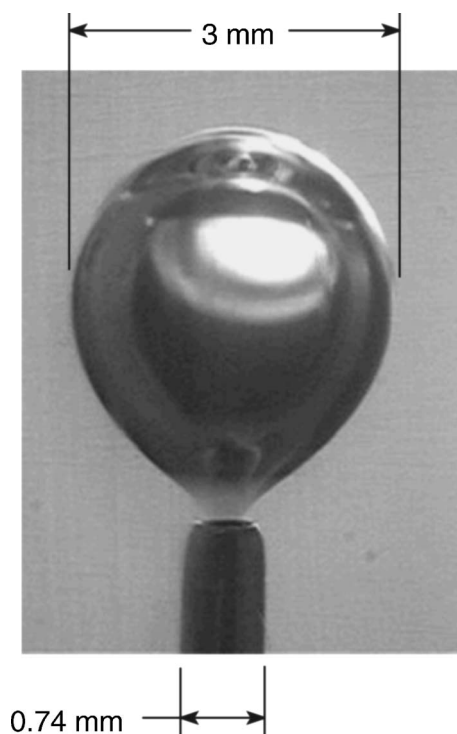


Fig. 3. A photograph of a typical bubble produced by one of the needles.

The acoustic energy is supplied by the bubbles themselves. When each individual bubble breaks off its needle, a transient acoustic pulse is produced. Continuous bubble production excites an acoustic standing wave field inside the waveguide that is observed with a hydrophone. A Brüel and Kjær model 8103 miniature hydrophone was used in this work, but a small lapel microphone can also be used.<sup>30</sup>

The hydrophone signal was amplified and bandpass filtered between 10 Hz and 10 kHz by a Brüel and Kjær model 2692 charge amplifier. The high-pass characteristic of the filter suppresses very low-frequency ( $<50$  Hz) flow noise, which can in some cases be dominant. Suppressing the flow noise allows the desired part of the signal (the eigenmodes of the waveguide) to be more easily heard by the audience. If the public address system has its own filter function, such as a graphic equalizer, a separate high-pass filter is not required. The low-pass filter was used for antialiasing the signal prior to digitization. If the apparatus is used solely for an audio demonstration, the low-pass filter is not required.

The hydrophone signal was directed to both a signal analyzer and a public address system. An Agilent 89410A vector signal analyzer (VSA) was used to digitize the conditioned hydrophone signal and display and record the spectrum of the signal via fast Fourier transform calculations performed onboard the VSA. Alternatively, a consumer-grade sound card can perform the same functions on many personal computers. Finally, the hydrophone signal must be amplified and directed to the loudspeaker system. We used a musical instrument amplifier designed for bass guitar, since the lowest eigenfrequencies can be below 100 Hz.

#### IV. DEMONSTRATION PROCEDURES

The PVC waveguide is filled with water and the hydrophone is placed midway down the tube. The exact placement

is not important at this stage.<sup>31</sup> The demonstration begins with no air flow from the needles, and hence, no bubbles in the waveguide. The VSA and the PA system are turned on and a flat spectrum of low amplitude is displayed, which gives an indication of the background noise in the room. The needle valve is then slowly opened to allow single bubbles to break off the needles one at a time. The individual breakoff events are audible through the PA system. Although not described here, the time series of the hydrophone signal could be presented using an oscilloscope. A bubble breakoff event would appear as a transient signal that approximates a damped sinusoid.

The flow rate is then slowly increased and a larger number of bubbles is created. The acoustic excitation becomes effectively continuous and standing waves develop in the waveguide. The excitation is sufficiently broadband to excite the first several normal modes of the waveguide. One can then continue to increase the flow rate and the number of bubbles further increases. This reduces the speed of sound in the waveguide, and hence reduces the frequency of the normal modes. As the flow rate continues to increase, the pitch of the sound produced continues to drop. Changing the void fraction via flow rate from 0.1% to 2% over a few seconds results in the speed of sound in the tube changing from approximately 300 m/s to 100 m/s over the same time scale, and hence the pitch of the sound is changed from about 150 Hz to 50 Hz, which is an octave and a half. This is easily detected by ear, but because the frequencies are relatively low, a large speaker is required to reproduce the sound. The overtones can still be heard if only a small speaker is available, but the demonstration is more effective with a large speaker.

As the flow rate is increased, the height of the water column also increases. This also plays a role in establishing the frequencies of the normal modes, but it is small compared to the variation due to the void fraction induced change in the speed of sound. In addition to ramping the flow rate up and then down, which produces decreasing and then increasing pitch, the user can vary the flow rate in any manner desired, which results in corresponding pitch changes. The user can also include a return to very low flow rates, which produces individual bubble breakoff events and their corresponding sounds. With some practice, one can achieve at times humorous, and at other times aesthetically pleasing and even musical sounds.

During the demonstration, the VSA displays the spectrum of the hydrophone signal in real time. Near the beginning of the demonstration, we establish a flow rate sufficiently high to yield continuous acoustic excitation, such as that shown in Fig. 4(a). The demonstrator can point out that the peaks in the spectra correspond to the eigenfrequencies of the waveguide and that these frequencies combine to produce the acoustic sound we perceive during the experiment. As the frequencies of these peaks increase, the pitch is also perceived by a listener to increase. The spectra of these sounds can be seen in real time on the signal analyzer, with the peaks shifting up and down with the flow rate. Ideally, a waterfall plot can be displayed showing a brief history, like that shown in Fig. 4(b). This demonstration has been performed by the authors many times to the approval of observers ranging from elementary school students to deans of large research universities.

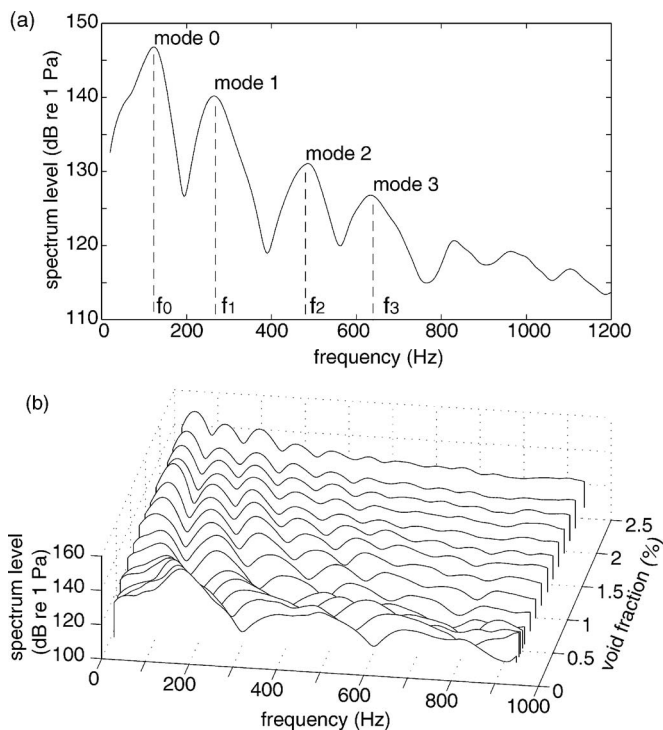


Fig. 4. (a) A single spectrum from the 0.4% void fraction case for which the individual modes and their eigenfrequencies  $f_n$  have been identified. The units are decibels (dB) referenced to  $1 \mu\text{Pa}$ , where  $\text{dB} = 20 \log_{10}[p/p_{\text{ref}}]$ ,  $p$  is the RMS acoustic pressure measured in the tube, and  $p_{\text{ref}} = 1 \mu\text{Pa}$ . (b) A waterfall plot of all the experimental spectra.

## V. VERIFICATION OF WOOD'S EQUATION

The bubbles produced in the apparatus are typically about 1 mm in radius, hence they have resonance frequencies near 3 kHz, according to Eq. (2). As long as the eigenfrequencies of the waveguide are well below the bubble resonance frequency, the bubbly liquid-filled waveguide will exhibit a speed of sound nearly independent of frequency and bubble size and the mixture will behave as an effective medium with a speed of sound given by Wood's equation [Eq. (12)].

To experimentally verify Eq. (12), spectra like the one shown in Fig. 4(a) are obtained for a range of air flow rates. At each flow rate, the height of the column  $L = \ell + \Delta\ell$  is measured using the float at the top of the waveguide and the void fraction  $\chi$  is determined from Eq. (18). Due to motion of the water surface, the uncertainty in  $\Delta\ell$  is about  $\pm 0.5$  mm, which leads to an uncertainty in the void fraction  $\chi$  of  $\pm 0.001$ . The bubble-free column height was  $\ell = 0.485 \text{ m} \pm 0.005 \text{ m}$ . A collection of spectra at void fractions ranging up to  $\chi = 2.5\%$  is shown in Fig. 4(b).

As indicated by Eq. (17), a plot of the modal frequencies versus mode number ideally yields a straight line with a slope directly proportional to the speed of sound in the bubbly liquid. Examples for three void fractions are shown in Fig. 5. A least squares linear fit of the measured resonance frequencies yields the slope from which the speed of sound is obtained for each void fraction. At higher void fractions,  $\chi = 2.46\%$  and  $0.6\%$ , the bubbles are approximately homogeneously spaced along the length of the tube, which yields an effective speed of sound that is constant throughout the tube. The resulting resonance frequencies are nearly harmonic. At the lower void fractions, exemplified by  $\chi = 0.13\%$ , the

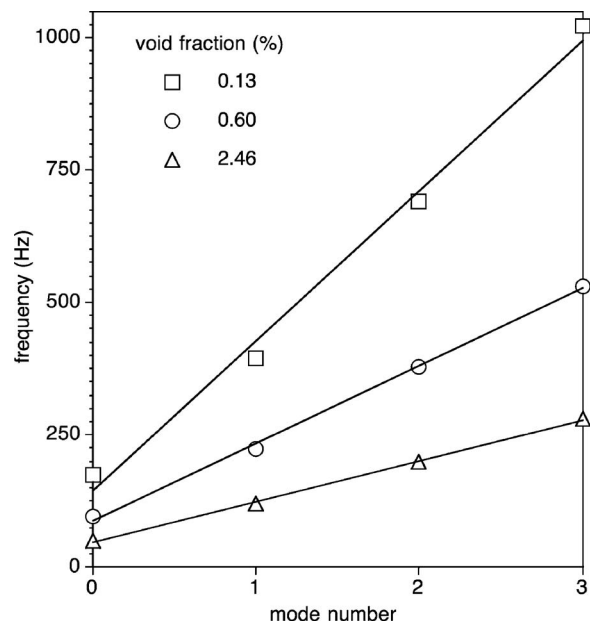


Fig. 5. Linear fits to the measured resonance frequencies as function of mode number for three void fractions: the lowest, the highest, and an intermediate void fraction.

bubbles are fewer in number and less homogeneously spaced throughout the tube. This results in a speed of sound that is inhomogeneous and resonance frequencies that are not perfectly harmonic, and hence less well-represented by a linear fit.

The speeds of sound thus inferred for the entire dataset are plotted versus void fraction in Fig. 6. Vertical error bars represent the uncertainty in the speed of sound due to uncertainties in the tube length,  $L$ ,  $\pm 1$  mm, and the finite bandwidth resolution of the spectra, which was 2.5 Hz. The solid line is Eq. (12) plotted using the following physical parameters:

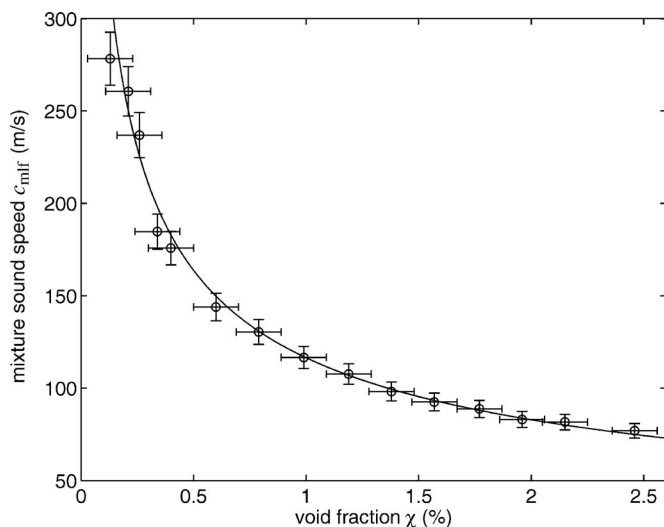


Fig. 6. Experimental verification of Wood's equation. The solid line is the prediction of Eq. (12) and the open circles are the measured values. Vertical error bars represent the uncertainties in the measurement of the speed of sound due to uncertainties in the column length  $L$  and the finite bandwidth resolution of the spectra. Horizontal error bars represent uncertainties in the void fractions due to the uncertainty in the measured values of  $\Delta\ell$ .

$\rho_\ell = 998 \text{ kg/m}^3$ ,  $\rho_g = 1.21 \text{ kg/m}^3$ ,  $c_\ell = 1494 \text{ m/s}$ , and  $c_g = 334 \text{ m/s}$ . The speed of sound in the liquid,  $c_\ell$ , was determined from the water temperature,  $24^\circ\text{C}$ , and Eqs. (5), (6), and (8) of Ref. 21. The speed of sound in the gas,  $c_g$ , was determined from Eqs. (7) and (10) for a hydrostatic pressure due to the standard atmospheric pressure,  $101.3 \text{ kPa}$ , and one half the column height of water,  $0.24 \text{ m}$ . Agreement within the measurement uncertainty is found between the measured and predicted speeds of sound throughout the range of void fractions. Below  $\chi = 0.3\%$ , the agreement is somewhat less than at higher void fractions. This is due to the inhomogeneous conditions inside the waveguide discussed before. The effective medium theory breaks down under such conditions and can no longer be used to describe the system. To investigate lower void fractions, a bubble injection scheme capable of evenly spacing bubbles at low flow rates would be required.

## VI. CONCLUSIONS

A simple laboratory apparatus is described that provides an audible demonstration of several aspects of the acoustics of bubbly liquids. The speed of sound in a bubbly liquid contained within a PVC pipe is altered by varying the injection rate of air bubbles. The bubble injection process itself produces broadband noise that excites one-dimensional standing waves within the apparatus. The variation of the speed of sound as a function of the void fraction is apparent in the associated change of the pitch of the sounds produced. The apparatus can also be used to verify an effective medium model of sound propagation in bubbly liquid, which relates the void fraction to the speed of sound.

## ACKNOWLEDGMENT

This work was supported by the U.S. Navy Office of Naval Research Ocean Acoustics Program.

<sup>a</sup>Electronic mail: pswilson@mail.utexas.edu

<sup>1</sup>A. Mallock, "The damping of sound by frothy liquids," *Proc. Royal Soc.* **84**(A 572), 391–395 (1910).

<sup>2</sup>Arnulph Mallock worked for Lord Rayleigh in the 1870s and conducted experiments in the hydraulic laboratory at Terling, Lord Rayleigh's estate, as discussed in R. J. Strutt, *Life of John William Strutt, Third Baron Rayleigh, O. M., F. R. S* (University of Wisconsin Press, Madison, 1968).

<sup>3</sup>L. Rayleigh, "On the pressure developed in a liquid during the collapse of a spherical cavity," *Philos. Mag.* **34**, 94–98 (1917).

<sup>4</sup>M. Minnaert, "On musical air-bubbles and the sounds of running water," *London, Edinburgh Dublin Philos. Mag. J. Sci.* **16**, 235–248 (1933).

<sup>5</sup>C. Crowe, M. Sommerfeld, and Y. Tsuji, *Multiphase Flows with Droplets and Particles* (CRC Press, Boca Raton, 1998).

<sup>6</sup>L. E. Faidley and J. A. I. Mann, "Development of a model for acoustic liquid manipulation created by a phased array," *J. Acoust. Soc. Am.* **109**(5), 2363 (2001).

<sup>7</sup>H. B. Karplus, "The velocity of sound in a liquid containing gas bubbles," Technical Report No. C00-248, Armour Research Foundation

of Illinois Institute of Technology (1958).

<sup>8</sup>H. Medwin and C. S. Clay, *Fundamentals of Acoustical Oceanography* (Academic Press, Boston, 1998).

<sup>9</sup>*Underwater Ship Husbandry Manual*, Naval Sea Systems Command, 1995, NAVSEA Publication S0600-AA-PRP-050.

<sup>10</sup>F. Calliada, R. Campani, O. Bottinelli, A. Bozzini, and M. G. Sommaruga, "Ultrasound contrast agents basic principles," *Eur. J. Radiol.* **27**, S157–S160 (1998).

<sup>11</sup>S. Vaezy, R. Martin, P. Mourad, and L. A. Crum, "Hemostasis using high intensity focused ultrasound," *Eur. J. Ultrasound* **9**, 79–87 (1999).

<sup>12</sup>X. Yang, R. A. Roy, and R. G. Holt, "Bubble dynamics and size distributions during focused ultrasound insonation," *J. Acoust. Soc. Am.* **116**(6), 3423–3431 (2004).

<sup>13</sup>H. C. Pumphrey and L. A. Crum, "Free oscillations of near-surface bubbles as a source of the underwater noise of rain," *J. Acoust. Soc. Am.* **87**(1), 142–148 (1990).

<sup>14</sup>J. H. Wilson, "Low-frequency wind-generated noise produced by the impact of spray with the ocean's surface," *J. Acoust. Soc. Am.* **68**(3), 952–956 (1980).

<sup>15</sup>L. A. Crum, H. C. Pumphrey, R. A. Roy, and A. Prosperetti, "The underwater sounds produced by impacting snowflakes," *J. Acoust. Soc. Am.* **106**(4), 1765–1700 (1999).

<sup>16</sup>W. M. Carey and J. W. Fitzgerald, "Low Frequency Noise from Breaking Waves," in *Natural Physical Sources of Underwater Sound*, edited by B. R. Kerman (Kluwer, Boston, 1993), pp. 277–304.

<sup>17</sup>F. S. Crawford, "The hot chocolate effect," *Am. J. Phys.* **50**(5), 398–404 (1982).

<sup>18</sup>S. Aljishi and J. Tatarkiewicz, "Why does heating water in a kettle produce sound?," *Am. J. Phys.* **59**(7), 628–632 (1991).

<sup>19</sup>V. Leroy, M. Devaud, and J.-C. Bacri, "The air bubble: Experiments on an unusual harmonic oscillator," *Am. J. Phys.* **70**(10), 1012–1019 (2002).

<sup>20</sup>K. W. Commander and A. Prosperetti, "Linear pressure waves in bubbly liquids: Comparison between theory and experiments," *J. Acoust. Soc. Am.* **85**(2), 732–746 (1989).

<sup>21</sup>L. E. Kinsler, A. R. Frey, A. B. Coppens, and J. V. Sanders, *Fundamentals of Acoustics*, 4th ed. (Wiley, New York, 2000).

<sup>22</sup>T. G. Leighton, *The Acoustic Bubble* (Academic Press, London, 1994).

<sup>23</sup>A. B. Wood, *A Textbook of Sound*, 1st ed. (MacMillan, New York, 1930).

<sup>24</sup>D.-Y. Hsieh and M. S. Plesset, "On the propagation of sound in a liquid containing gas bubbles," *Phys. Fluids* **4**(8), 970–975 (1961).

<sup>25</sup>A. Prosperetti, "The thermal behavior of oscillating gas bubbles," *J. Fluid Mech.* **222**, 587–616 (1991).

<sup>26</sup>A. Crespo, "Sound and shock waves in liquids containing bubbles," *Phys. Fluids* **12**(11), 2274–2282 (1969).

<sup>27</sup>A. E. Ruggles, H. A. Scarton, and R. T. Lahey Jr., "An Investigation of the Propagation of Pressure Perturbations in Bubbly Air/Water flows," in *First International Multiphase Fluid Transients Symposium*, edited by H. H. Safwat, J. Braun, and U. S. Rohatgi (American Society of Mechanical Engineers, New York, 1986), pp. 1–9.

<sup>28</sup>D. T. Blackstock, *Fundamentals of Physical Acoustics* (Wiley, New York, 2000).

<sup>29</sup>Hamilton Company; 4970 Energy Way; Reno, Nevada 89502 USA. <http://www.hamiltoncompany.com/>

<sup>30</sup>The lapel mic must be made water proof. This can be done by coating the microphone with rubber, such as Plasti Dip, available at hardware stores. [http://www.plastidip.com/home\\_solutions/Plasti\\_Dip](http://www.plastidip.com/home_solutions/Plasti_Dip)

<sup>31</sup>The field inside the waveguide is spatially dependent according to Eq. (16). One can accentuate or suppress a mode by placing the hydrophone near an antinode or a node, respectively. Since the excitation is broadband, a number of modes are excited, but the relative amplitude of a particular mode received on the hydrophone depends on the hydrophone's location inside the waveguide.